TOXICOLOGICAL SCIENCES **116(2)**, 604–613 (2010)
doi:10.1093/toxsci/kfq139
Advance Access publication May 13, 2010

Allethrin Differentially Modulates Voltage-Gated Calcium Channel Subtypes in Rat PC12 Cells

April P. Neal, Yukun Yuan, and William D. Atchison[1]

Department of Pharmacology and Toxicology, Michigan State University, East Lansing, Michigan 48824-1317

[1]To whom correspondence should be addressed at Department of Pharmacology and Toxicology, Michigan State University, B-331 Life Sciences Building, East Lansing, MI 48824-1317. Fax: (517) 432-1341. E-mail: atchiso1@msu.edu.

Received March 4, 2010; accepted May 4, 2010

Pyrethroid insecticides are one of the most widely used classes of insecticides. Previous studies revealed that pyrethroids potently affect the insect voltage-gated sodium (Na^+) channel (VGSC), resulting in prolonged channel open time. However, recent findings have suggested that pyrethroids may affect targets other than the VGSC. In particular, several studies have shown that pyrethroids can modulate the activity of voltage-gated calcium (Ca^{2+}) channels (VGCCs). However, these studies often reported conflicting results; some studies observed stimulatory effects, whereas others observed inhibitory effects of pyrethroids on VGCCs. This study investigated whether allethrin (AL), a well-characterized type I pyrethroid, altered VGCC characteristics measured by whole-cell recording in rat pheochromocytoma cells (PC12) differentiated with nerve growth factor (NGF). AL (5μM) increased peak, end, and tail composite VGCC current independent of its effects on VGSCs. After blocking VGCC subtype–specific current with ω-conotoxin GVIA (GVIA, an N-type VGCC antagonist) or nimodipine (NIM, an L-type VGCC antagonist), our data further suggest that AL differentially affects VGCC subtypes. Thus, AL apparently stimulated GVIA-insensitive current while inhibiting NIM-insensitive current. AL also significantly altered the voltage dependency of activation and inactivation of L-type VGCCs. The differential modulation of VGCC subtypes by AL may explain some of the conflicting observations of other studies.

Key Words: **allethrin; pyrethroids; voltage-gated calcium channel; PC12 cells; voltage-gated sodium channel; neurotoxicity induced.**

Pyrethroid insecticides are one of the most widely used classes of insecticides. Since the worldwide reduction in use of chlorinated pesticides, such as dichlorodiphenyltrichloroethane (DDT), pyrethroids have been essential in controlling disease-carrying vectors in tropical climates (Zaim and Jambulingam, 2010). They also comprise a major component of pesticide use in the United States (Department of Health and Human Services, 2009; U.S. Environmental Protection Agency, 2006a, 2006b). Pyrethroid insecticides immobilize insects by promoting the open state of the insect voltage-gated sodium (Na^+) channel (VGSC) and delaying channel inactivation, resulting in a prolonged depolarizing tail current that can lead to increased excitability (Narahashi, 1986; Ray and Fry, 2006).

There are two classes of pyrethroids differentiated by the presence of a cyano group: type II compounds have this cyano group, whereas type I agents do not. The two classes cause different toxicological symptoms likely because of differences in their effects on neurons. Although significant heterogeneity exists, type II pyrethroids generally prolong VGSC open time more than type I pyrethroids (Ray and Fry, 2006). Whereas type I poisonings cause whole-body tremor, exaggerated startle response, and hyperexcitability in mammals (Narahashi, 1986; Ray and Fry, 2006; Shafer and Meyer, 2004), type II poisonings cause a more complex series of symptoms, including excessive salivation, uncoordination, and generalized choreoathetosis (Ray and Fry, 2006).

Differences in the toxicity of the two compounds prompted studies to investigate whether pyrethroids have targets other than the VGSC. These suggest that both type I and type II pyrethroids interact with voltage-gated calcium (Ca^{2+}) channels (VGCCs). VGCCs share many similar characteristics to VGSCs, such as multimeric structure, a common pore motif, and pore-opening and gating mechanisms (Catterall *et al.*, 2007). Several studies have noted effects of pyrethroids on VGCCs in the same concentration range as their effects on VGSCs (Ginsburg and Narahashi, 1999; Hildebrand *et al.*, 2004; Vais *et al.*, 2001). Increased neurotransmitter release from synaptosomes has been observed during exposure to type II pyrethroids (Clark and Symington, 2008), presumably as a result of increased intracellular Ca^{2+} levels. These studies also suggested that the N-type VGCC was more sensitive to pyrethroid exposure than other synaptic VGCC subtypes because selective inhibition of N-type VGCCs abolished the effects on transmitter release (Clark and Symington, 2008; Symington *et al.*, 2007b). In hippocampal neurons, exposure to a type I pyrethroid (permethrin) resulted in a Ca^{2+}-dependent increase in miniature excitatory postsynaptic current (mEPSC)

frequency in the presence of tetrodotoxin (TTX), a VGSC-specific antagonist. In contrast, a type II pyrethroid (deltamethrin [DM]) did not affect mEPSC frequency under these conditions (Meyer and Shafer, 2006). In HEK293 cells expressing recombinant VGCCs, the type I pyrethroid allethrin (AL) potently blocked L-, P/Q-, and T-type VGCCs in a subtype-independent manner with IC_{50}s of 6.7–7.0μM (Hildebrand *et al*., 2004). These are equivalent to those needed for AL to affect insect or mammalian VGSCs (Ginsburg and Narahashi, 1999; Wang, 1972). Thus, although studies agree that pyrethroids affect VGCCs, many inconsistencies prevent a clear picture of the mode of action.

To help clarify the effects of pyrethroids on VGCCs, we examined the effects of a well-studied type I pyrethroid, AL, on VGCCs expressed in differentiated rat pheochromocytoma (PC12) cells. PC12 cells are derived from the rat adrenal medulla but develop a sympathetic neuron phenotype when differentiated with nerve growth factor (NGF) (Garber *et al*., 1989; Shafer and Atchison, 1991). This cell line has been used extensively in neurotoxicological studies (Shafer, 1998; Shafer and Atchison, 1991; Shafer *et al*., 2005a; Tillar *et al*., 2002) and is a reliable system in which to study the effects of neurotoxicants on voltage-gated ion channels. We observed that AL differentially modulates VGCC subtypes, which may help explain contradictory results of previous studies.

MATERIALS AND METHODS

Chemicals and solutions. Allethrin (AL, 33396, mixed isomers), nimodipine (NIM), and ω-conotoxin GVIA (GVIA) were obtained from Sigma–Aldrich (St Louis, MO). RPMI Medium 1640 (RPMI), fetal bovine serum, and horse serum were obtained from Invitrogen (Carlsbad, CA). AL working solutions (5 and 20μM) were made on the day of use in extracellular recording solution (in millimolars: 20 $BaCl_2$, 20 4-(2-Hydroxyethyl)piperazine-1-ethanesulfonic acid [HEPES], 1 $MgCl_2$, 95 NaCl, 10 tetraethylamonium chloride [TEACl], and 10 dextrose, pH 7.4 with NaOH at 23°C–25°C) from a 50mM stock solution of AL dissolved in dimethyl sulfoxide (DMSO). The concentration of DMSO in working AL solutions did not exceed 0.1% (vol/vol). AL and NIM solutions were wrapped with foil to avoid photodegradation. The pipette solution consisted of (in millimolars) 2 ATP-Mg^{2+}, 125 CsCl, 5 ethylene glycol-bis(2-aminoethylether)-*N*,*N*,*N*′,*N*′-tetraacetic acid (EGTA), 10 dextrose, 10 HEPES, 10 TEACl, pH 7.4 at 23°C–25°C with tetraethylammonium hydroxide. TTX (Sankyo, Tokyo, Japan) was stored in deionized water, NIM was stored in DMSO, and final concentrations are given in the "Results" section.

PC12 cell culture. PC12 cells (gift of Dr M. L. Contreras, formerly of Michigan State University) used in these studies were from passages 23–31 from our receipt. Cells were grown in RPMI medium plus 7.5% (vol/vol) fetal bovine serum and 7.5% (vol/vol) horse serum (PC12 medium). For recording, 1.5×10^6 cells were seeded in 35-mm plates (Corning, Corning, NY) in PC12 medium. Two hours after plating, the medium was replaced with PC12 medium containing 100 ng/ml mouse 7s NGF (gift of Dr M. L. Contreras). Cells were grown for 5–7 days in PC12 medium containing 100 ng/ml NGF with medium exchange every 3rd or 4th day.

Electrophysiological recording. Cells grown in 35-mm plates as described above were continuously perfused at 1 ml/min with extracellular solution using a setup similar to that described by Tatebayashi and Narahashi (1994). Ba^{2+} (20mM) was used as the charge carrier in all experiments. Borosilicate glass capillaries (inner diameter [ID] 0.68 mm, outer diameter [OD] 1.2 mm, length 100 mm; World Precision Instruments, Sarasota, FL) were used in place of rubber tubing for perfusion to prevent contamination of tubing by AL. The volume of the recording chamber was ~500 μl. Patch electrodes were pulled using a Flaming/Brown pipette puller (Sutter Instrument Co, Novato, CA) from borosilicate glass capillaries (ID 1.0 mm, OD 1.5 mm; Harvard Apparatus, Holliston, MA) and fire polished to 2–7 MΩ when filled with the above solution. Ca^{2+} currents were recorded in the whole-cell configuration using an Axopatch 200B amplifier (Molecular Devices-Axon Instruments, Sunnyvale, CA). Data were acquired using a PC-compatible computer equipped with a Digidata 1322A interface and pCLAMP software (version 9.2; Axon Instruments).

Whole-cell currents were filtered at 1–2 kHz with an 8-pole low-pass Bessel filter and digitized at 20 kHz for off-line analysis. Ca^{2+} currents were activated either using a ramp depolarization from −100 to 60 mV with a steady-state holding potential of −80 mV or from a holding potential of −70 mV using 200 ms test pulses from −60 to +60 mV in 10-mV increments. Inactivation curves were obtained by stepping 200 ms test pulses of 0 mV from holding potentials, which varied from −70 to 0 mV in 10-mV increments. The magnitude of tail currents was assessed from the current present after repolarization to −70 mV from a 200 ms test pulse at 0 mV. Control recordings were performed in extracellular solution in the absence of AL but with equivalent levels of DMSO as the treated condition. These recordings were followed by recordings from the same cell during continuous perfusion with extracellular solution containing AL. VGCC currents from AL-exposed cells were recorded 3 min after the exchange to AL-containing extracellular solution. One cell was recorded from a single culture dish and was considered an independent measure; a total of 5–6 cultures were used for each treatment condition for n = 5–6. After AL exposure, the aspirator tip and ground electrode were bathed for 5 min in NaOH solution (0.25 M) to promote AL degradation and cleaned with 70% ethanol before the next use. All glassware was exchanged between recordings of AL-treated cells.

Voltage-dependency of activation was determined using the Boltzman equation: $G/G_{max} = 1/(1 + e^{-(V - V50)/k})$, where V_{50} is the half-activation potential and k is a measure of steepness. Chord conductance (G) was calculated by the equation: I/(driving force), where I is the current present during the test potential and the driving force is the result of the test potential minus the reversal potential observed for that cell. G at each test potential ranging from −70 to + 20 mV in 10-mV steps was divided by the maximum conductance (G_{max}) to yield normalized conductance (G/G_{max}).

Voltage-dependency of inactivation was determined using the Boltzman equation: $I/I_{max} = 1/(1 + e^{-(V - V50)/k})$, where V_{50} is the half-inactivation potential and k is a measure of steepness. The inactivation protocol followed a two-pulse design; first, the cell was subjected to a depolarizing pulse ranging from −70 to 0 mV in 10-mV increments lasting 200 ms. Then, the cell was immediately subjected to a test pulse at 0 mV for 200 ms. Normalized current (I/I_{max}) was obtained by dividing the current observed at the test pulse by the maximum current observed.

Activation rate values (τ_{act}) were determined by measuring the rising phase to peak current during depolarization to 0 mV from a holding potential of −70 mV. Inactivation time constant (τ_{inact}) values were determined by the falling phase from peak current to baseline. The τ values of the tail currents (τ_{deact}) were assessed by fitting the peak tail current present after repolarization from a 200 ms test pulse at 0 to −70 mV to the subsequent steady-state period using a single exponential model. A single exponential model fit all decay phases (not shown) and was used to estimate τ_{act}, τ_{inact}, and τ_{deact} (pCLAMP, version 9.2).

Peak current was measured as the maximum current present during step depolarizations. End current was measured as the amplitude of current remaining at the end of the 200 ms test pulses. Peak tail current was measured as the maximum current present after repolarization to −70 mV from a test potential of 0 mV.

Statistics. Peak current, peak tail current, and end current were normalized to the matched control, averaged, and subjected to paired *t*-test analyses (Sigmaplot Version 11.0; Systat, Chicago, IL). Values of $p < 0.05$ were considered to be statistically significant.

RESULTS

Allethrin Exposure Increases Peak, End, and Tail VGCC Current

We investigated the effects of AL on VGCC electrophysiological properties in PC12 cells differentiated via exogenous addition of mouse NGF. Undifferentiated PC12 cells predominately express only L-type VGCC. When differentiated using NGF, PC12 cells acquire a neuronal phenotype and express T-, N-, L- and P/Q-type VGCCs, albeit with varying levels of expression (del Toro *et al.*, 2003; Garber *et al.*, 1989; Shafer and Atchison, 1991). AL increased whole-cell VGCC currents induced by a ramp depolarization from −100 to 60 mV from a holding potential of −80 mV (Fig. 1). These effects appeared to be concentration-dependent (Fig. 1A) and were not due to interaction of AL with the VGSC because we observed similar effects in the presence of 0.5μM TTX (Fig. 1B). AL can modulate TTX-insensitive VGSCs (Ginsburg and Narahashi, 1999), but we did not observe any residual whole-cell current after addition of 100μM Cd^{2+}, a nonspecific VGCC blocker. These results suggest that TTX-insensitive VGSCs, if present, do not constitute a significant proportion of whole-cell current in these cells.

We chose to examine the effects of 5μM AL for this study because this concentration is within the range that AL modified VGSCs and VGCCs in other studies (Ginsburg and Narahashi, 1999; Hildebrand *et al.*, 2004; Narahashi, 1986). Figures 1C–F show representative current traces recorded during a 200-ms test depolarizing pulse of 0 mV from a holding potential of −70 mV. We observed that the peak, end, and tail current magnitudes appeared to increase during exposure to 5μM AL (Figs. 1C and 1D). These effects were observed in the presence of TTX, indicating they are mediated by VGCCs (Figs. 1E and 1F). Subtraction of control from treated current reveals the current stimulated by AL (AL-stimulated, Figs. 1C and 1E). This current appears to exhibit both slow activation and inactivation and was similar in cells with or without TTX treatment.

These qualitative observations led us to examine AL effects on VGCC current more closely. Figure 2 shows the effect of AL on VGCC peak and end current-voltage relationships (I-V curves) as well as the effect of AL on the magnitude of peak, end, and tail VGCC current. AL shifted the peak and end current-voltage relationships (I-V curves) to more hyperpolarized potentials, from 10 to 0 mV (Figs. 2A–D). The AL-stimulated current was maximally stimulated at −10 mV for peak current and 0 mV for end current. These effects were observed in cells irrespective of the presence of 0.5μM TTX, indicating that AL is mediating these effects through interaction with VGCCs. Maximum peak and end current during AL exposure was significantly increased (Figs. 2E and 2F), and so was the magnitude of tail current present after repolarization to −70 mV from a test potential of 0 mV (Fig. 1).

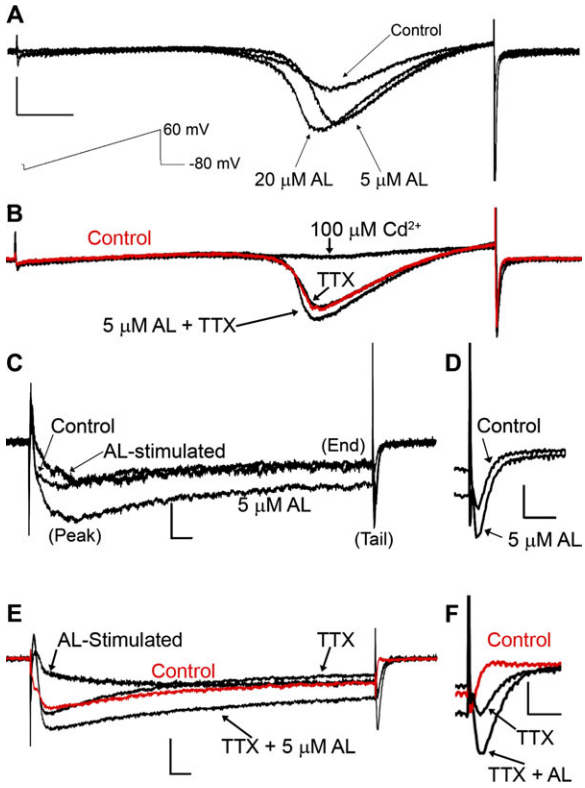

FIG. 1. Allethrin-sensitive currents are mediated by VGCCs in differentiated PC12 cells. (A and B) A large inward current was induced during a ramp depolarization from −100 to 60 mV from a holding potential of −80 mV. (A) The amplitude of this current was increased by addition of 5 or 20μM AL. (B) Increased current was observed in the presence of 0.5μM TTX and abolished by 100μM Cd^{2+}, a nonspecific VGCC blocker. Control trace (no TTX or AL) is nearly identical to the TTX trace. This indicates that the AL-increased current is mediated by VGCCs. The scale in (A) also represents (B) vertical = 150 pA, horizontal = 20 ms. Stimulus protocol for (A) and (B) is shown beneath scale bars in (A) (not in scale). (C and F) Whole-cell currents of VGCCs in PC12 cells were evoked by stepping a 200-ms depolarizing pulse to 0 mV from a holding potential of −70 mV. (C) Traces were recorded before and during incubation with 5μM AL. Subtraction of control from treated results in AL-stimulated current. Peak, end, and tail currents are labeled for reference. (D) Magnified view of control and 5μM AL tail current from (C). (E) Traces recorded before and during incubation with 5μM AL in the presence of 0.5μM TTX. (F) Magnified view of TTX and TTX + 5μM AL tail current from (E). The scale in (C) and (E) is horizontal = 10 ms, vertical = 100 pA; for (D) and (F): horizontal = 4 ms, vertical = 100 pA.

Allethrin Does Not Significantly Affect Voltage Dependency or Rates of Activation, Inactivation, or Deactivation of Composite VGCC Current

The shift in the I-V curves of whole-cell currents during AL exposure (Fig. 2) prompted us to examine VGCC activation and inactivation in isolation. We did not observe a significant effect of AL on the half-activation voltage (V_{50}) or the steepness (k) of the activation curve (Figs. 3A and 3B and Table 1). Similarly, we did not observe a significant effect of AL on the V_{50} or steepness of VGCC inactivation (Figs. 3C and 3D and Table 2). Using model fitting (see "Materials and

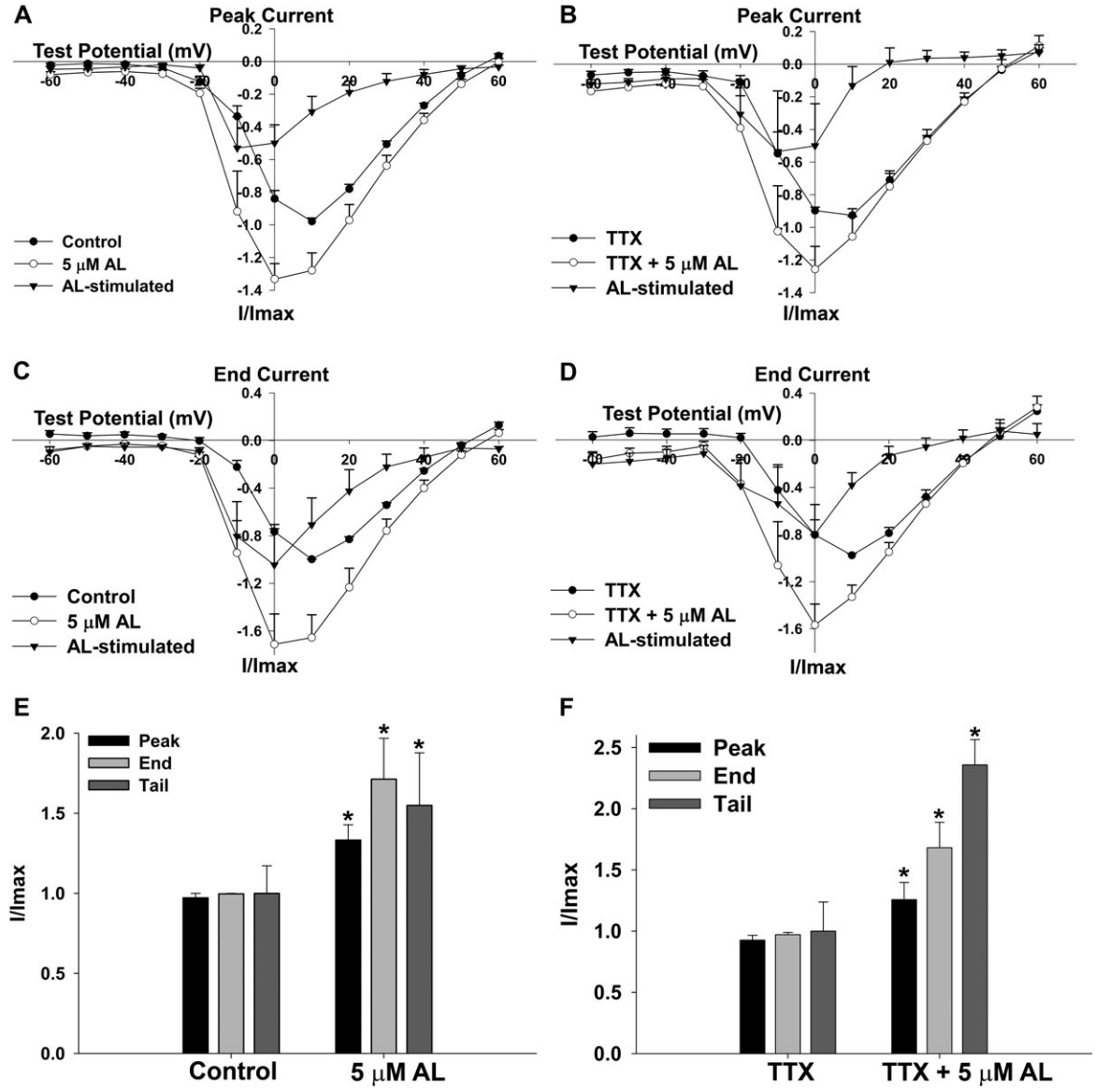

FIG. 2. Allethrin increases peak, end, and tail VGCC current and shifts the current-voltage relationships (I-V curves) to more hyperpolarized potentials. (A and B) I-V curves of peak currents for cells exposed to AL in the absence (A, $n = 6$ cells) or presence (B, $n = 5$ cells) of 0.5μM TTX. Maximum peak current is shifted from 10 to 0 mV in both cases. The peak AL-stimulated current maximizes at −10 mV. (C and D) I-V curves of end currents for cells exposed to AL in the absence (C, $n = 6$ cells) or presence (D, $n = 5$ cells) of 0.5μM TTX. Maximum end current is shifted from 10 to 0 mV, and the AL-stimulated current exhibits maximum amplitude at 0 mV. (E–F) Peak and end currents represent the maximum values from (A–D), which occurred at 10 mV before AL exposure and 0 mV after AL exposure. Tail current represents the magnitude of the tail current present after repolarization to −70 mV from a test potential of 0 mV (Fig. 1). All three parameters of VGCC current increased during AL exposure, even in the presence of 0.5μM TTX. Data were analyzed by paired *t*-test, $n = 6$ cells for (E) and $n = 5$ cells for (F). The asterisk depicts a statistically significant difference ($p < 0.05$).

Methods" section), we did not observe any AL-induced differences in the rate of activation (τ_{act}), inactivation (τ_{inact}), or deactivation (τ_{deact}) (Table 3).

The Shift in Peak and End I-V Curves by AL Is Mediated by Interaction with L-type VGCCs

Recent publications have suggested that VGCC subtypes may exhibit different sensitivities to pyrethroids. N-type VGCCs ($Ca_v2.2$) have been postulated to be particularly sensitive to pyrethroid exposure in rat brain synaptosomes and *Xenopus laevis* oocyte expression systems (Clark and Symington, 2008; Symington *et al.*, 2007a). To determine if the effects of AL observed in this study are a result of AL interaction with specific VGCC subtypes, we pharmacologically isolated different current types. N-type VGCC current was blocked by pretreating PC12 cells with 1μM ω-conotoxin GVIA

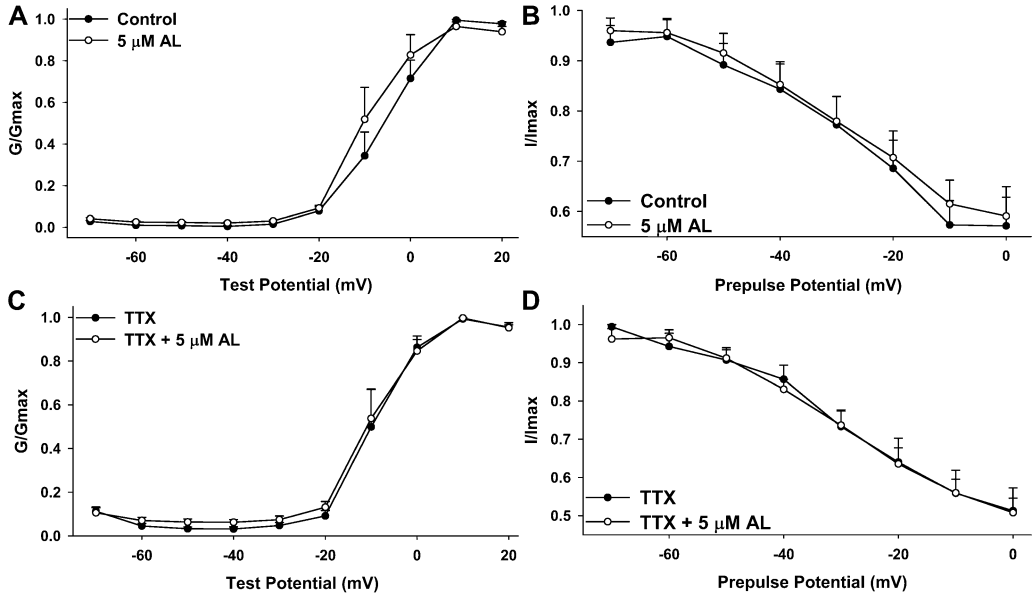

FIG. 3. Allethrin does not significantly affect voltage dependency of activation or inactivation of whole-cell VGCC current. Activation curves (A and C) were generated by normalizing the conductance observed at test pulses from −70 to + 20 mV to the maximum conductance. For inactivation curves (B and D), cells were subjected to a 200-ms prepulse at potentials ranging from −70 to 0 mV before testing VGCC current response at 0 mV. The current observed during the test pulse was normalized to the maximum current obtained. No significant effect was observed on the voltage dependency of activation or inactivation during exposure to AL (also see Tables 1 and 2).

(GVIA), a specific antagonist of N-type VGCCs. In a separate set of cells, we blocked L-type VGCCs current by adding 5μM NIM, a dihydropyridine-type (L-type) VGCC antagonist, to the extracellular solution before and during treatment with 5μM AL. Differences in antagonist exposure were based on the relatively irreversible binding of GVIA to N-type channels as compared with the reversible interaction of NIM with L-type VGCCs. The majority (~70%) of current was abolished by GVIA pretreatment (Fig. 4A), whereas ~20% of the current was blocked by NIM (Fig. 4B). Thus, N-type VGCCs are responsible for the majority of the current observed in our PC12 cells at this stage of differentiation. The remaining proportion of the current, roughly 10%, is likely derived from P/Q-, T-, and/or R-type VGCCs.

AL increased peak, end, and tail currents in cells pretreated with GVIA but actually decreased peak and end currents in cells treated with NIM (Fig. 4). This suggested that AL exerts differential effects on VGCC subtypes. When we examined the

TABLE 1
Voltage-Dependent Activation Parameters in PC12 Cells

	V_{50} (mV)	k
Control	−5.5 ± 2.5	4.7 ± 0.5
5μM AL	−9.5 ± 3.4	3.8 ± 1.0
TTX	−9.9 ± 2.9	3.2 ± 1.4
TTX + AL	−8.6 ± 2.6	5.1 ± 1.3
GVIA	−6.2 ± 3.1	4.8 ± 0.7
GVIA + AL	−12.0 ± 3.5[a]	5.2 ± 0.4
NIM	−2.1 ± 3.5	3.6 ± 0.9
NIM + AL	−0.90 ± 3.4	4.4 ± 0.5

Note. Parameters were estimated using the Boltzman equation ($G/G_{max} = 1/(1 + e^{-(V - V50)/k})$), where V_{50} is the half-activation voltage and k is a measure of steepness. No significant differences were observed within treatments, except that cells exposed to both GVIA and AL exhibited activation at a significantly more negative potential than cells exposed to GVIA alone. Values are reported as the mean ± SEM, n = 5–7 cells per condition.

[a]Significance from GVIA-treated cells ($p < 0.05$, paired t-test).

TABLE 2
Voltage-Dependent Inactivation Parameters in PC12 Cells

	V_{50} (mV)	k
Control	−0.1 ± 5.4	−32.6 ± 9.2
5μM AL	0.8 ± 5.2	−36.4 ± 8.3
TTX	−9.5 ± 9.4	−29.8 ± 4.9
TTX + AL	−9.8 ± 5.5	−31.2 ± 6.3
GVIA	40.4 ± 10.3[a]	−40.6 ± 17.3
GVIA + AL	−1.0 ± 7.4[b]	−45.3 ± 9.6
NIM	−13.4 ± 2.4	−27.8 ± 2.6
NIM + AL	−11.6 ± 3.9	−20.2 ± 5.0

Note. Parameters were estimated using the Boltzman equation ($I/I_{max} = 1/(1 + e^{-(V - V50)/k})$), where V_{50} is the half-inactivation voltage and k is a measure of steepness. No significant differences were observed within treatments, except that cells exposed to both GVIA and AL exhibited inactivation at a significantly more negative potential than cells exposed to GVIA alone.

[a]Extrapolated V_{50} of inactivation, as full inactivation is likely only theoretical under these conditions. Values are reported as the mean ± SEM, n = 5–7 cells per condition.

[b]Significance from GVIA-treated cells ($p < 0.05$, paired t-test).

TABLE 3
Allethrin Does Not Significantly Affect Activation, Inactivation, or Deactivation Rate Constants (τ) under Any Condition Tested

	τ_{act} (ms)	τ_{inact} (ms)	τ_{deact} (ms)
Control	4.7 ± 0.8	82.1 ± 10.3	3.1 ± 0.8
5μM AL	6.2 ± 0.9	114.2 ± 24.9	3.1 ± 0.9
TTX	4.1 ± 1.1	114.5 ± 21.1	4.3 ± 0.9
TTX + 5μM AL	4.2 ± 0.5	177.4 ± 45.7	3.5 ± 1.2
GVIA	4.3 ± 1.9	225.4 ± 78.7	2.3 ± 0.6
GVIA + 5μM AL	4.3 ± 0.8	253.8 ± 88.1	2.2 ± 0.5
NIM	4.5 ± 0.7	123.1 ± 20.0	3.3 ± 1.0
NIM + 5μM AL	4.7 ± 0.4	104.7 ± 19.0	2.9 ± 0.8

Note. See ''Materials and Methods'' section for description of estimation of τ. No significant differences were observed in any of the rate constants (ANOVA, $p > 0.05$), although GVIA treatment resulted in slower τ_{inact}, consistent with an increased proportion of L-type current, which inactivates more slowly than other VGCC subtypes. Values are reported as the mean ± SEM, $n = 5$–7 cells per condition.

effects of AL on peak and end I-V curves (Figs. 5A–D), we observed that cells pretreated with GVIA exhibited a similar shift toward hyperpolarized potentials as initially observed with composite VGCC currents (Fig. 2). However, cells treated with NIM did not exhibit a shift in the I-V curves of either peak or end current (Figs. 5B and 5D). Thus, the shift toward hyperpolarized potentials in peak and end I-V curves by AL was mediated by interaction with L-type VGCCs.

Allethrin Differentially Alters Peak and End Current Magnitudes of Subtype-Specific VGCCs

Whereas GVIA-treated peak and end current magnitudes increased, NIM-treated peak and end current magnitudes decreased during AL exposure (Figs. 5E and 5F). We analyzed these VGCC current parameters as described above for Figure 2. No significant effect was observed on tail current amplitude in cells treated with NIM during AL exposure. Thus, N-type channels are inhibited and L-type channels are stimulated by AL, with unknown effects on other high voltage–activated VGCCs.

Allethrin Shifts the Maximum Activation and Inactivation of L-type VGCCs to More Hyperpolarized Potentials but Does Not Alter Activation, Inactivation, or Deactivation Rate Constants

We next examined the activation and inactivation curves of VGCCs in cells pretreated with GVIA or continuously exposed to NIM. We observed a significant shift of about 6 mV in the V_{50} of activation during AL exposure in cells pretreated with GVIA. In contrast, NIM-treated activation was unaffected (Figs. 6A and 6C and Table 1). Thus, the shift in maximum voltage-dependent activation by AL was most likely mediated by interaction with L-type VGCCs, as it was absent in the presence of NIM. Similarly, the extrapolated V_{50} of VGCC inactivation in cells pretreated with GVIA was shifted by 40 mV, whereas that for cells treated with NIM was unaffected (Figs. 6B and 6D and Table 2). This again suggests that the shift in voltage-dependent inactivation observed with GVIA-treated cells exposed to AL was mediated by interaction with L-type VGCCs. No significant effect was observed on τ_{act}, τ_{inact}, or τ_{deact} of cells treated with either NIM or GVIA and exposed to AL (Table 3), suggesting that while both voltage-dependent activation and inactivation of L-type VGCCs were significantly shifted, the rates of activation and inactivation were unchanged.

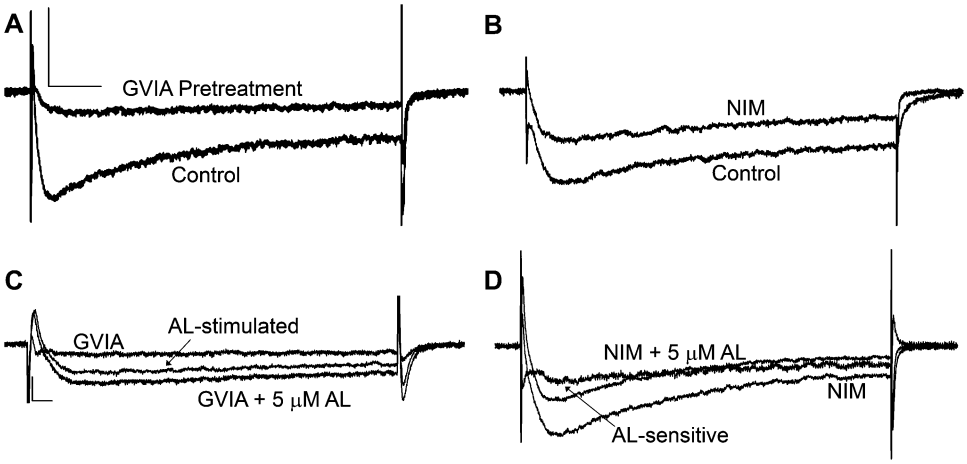

FIG. 4. Allethrin differentially modulates VGCC subtypes. PC12 cells were either pretreated with 1μM ω-conotoxin GVIA (GVIA) immediately before electrophysiological recording or continuously perfused with 5μM NIM during recording. (A) Blocking N-type VGCCs with GVIA reduces PC12 VGCC current by 70% relative to control recordings obtained on the same day. The scale in (A) applies to (B). The horizontal bar = 20 ms and the vertical bar = 200 pA. (B) Blocking L-type VGCCs with NIM reduces PC12 VGCC current by 20% compared with matched control recordings obtained before addition of NIM. (C) Exposure of GVIA-treated cells to 5μM AL appears to increase peak, end, and tail VGCC currents. The scale in (C) applies to (D). The horizontal bar = 10 ms and the vertical bar = 100 pA. (D) Simultaneous exposure of cells to NIM and 5μM AL appears to reduce peak and end current.

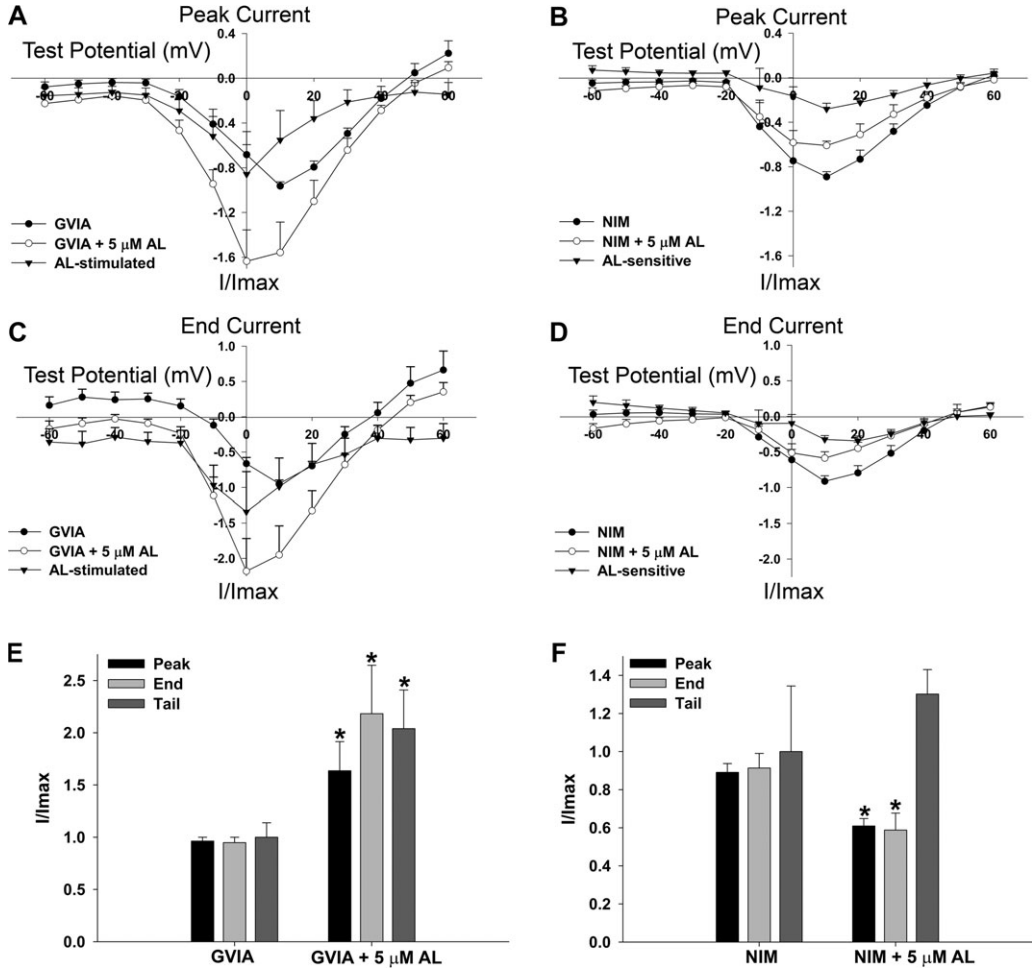

FIG. 5. Shift in peak and end VGCC I-V curves is because of AL interaction with L-type VGCCs. (A and B) I-V curves of peak currents for cells exposed to AL following pretreatment with GVIA (A, $n = 6$ cells) or continuous perfusion with NIM (B, $n = 5$ cells). Peak current is shifted from 10 to 0 mV in GVIA-treated cells but not in NIM-treated cells. The peak AL-stimulated current maximizes at 0 mV in GVIA-treated cells. NIM-treated cells exhibited an apparent decrease in peak current during exposure to AL, with maximum AL-sensitive current at 10 mV. (C and D) I-V curves of end currents for cells exposed to AL following pretreatment with GVIA (C) or continuous perfusion with NIM (D). Maximal end current is shifted from 10 to 0 mV, and the AL-stimulated current exhibits maximum magnitude at 0 mV in GVIA-treated cells. NIM-treated cells exhibited an apparent decrease in end current, with maximum AL-sensitive current at 10–20 mV. (E and F) Peak and end currents represent the maximum values from (A–D). Tail current represents the magnitude of the tail current measured after repolarization to −70 mV from a test potential of 0 mV. All three parameters of VGCC current were increased during AL exposure in GVIA-treated cells (E), whereas AL mediated a reduction of peak and end current in NIM-treated cells (F). Data were analyzed by paired *t*-test, $n = 7$ cells for (E) and $n = 5$ cells for (F). The asterisk depicts a statistically significant difference ($p < 0.05$).

DISCUSSION

Our observations regarding the effects of AL on VGCC currents in differentiated PC12 cells support the following conclusions. First, AL exposure results in a net increase in peak, end, and tail VGCC currents but differentially modulates VGCC subtypes. Second, AL preferentially shifts the peak current observed for GVIA-insensitive current to hyperpolarized potentials with altered voltage-dependency of activation and inactivation but does not affect the rate of VGCC activation, inactivation, or deactivation under any of the conditions tested.

Though unique in subunit structure, there are fundamental similarities between VGCCs and VGSCs. Both contain a pore-forming α subunit, accessory β subunits, and similar gating mechanisms, although the VGCC has additional α2δ and γ subunits (Catterall *et al.*, 2007). However, the effects we observed with AL on VGCC currents differ from those previously described for the effects of AL on VGSC currents, even though the effects occurred within the same concentration range. Narahashi (1986) observed that 1μM AL applied to squid axon increased the steady-state (end) and tail current and slowed tail current decay but had no effect on peak current. In rat dorsal root ganglion (DRG) cells, 10μM AL increased tail

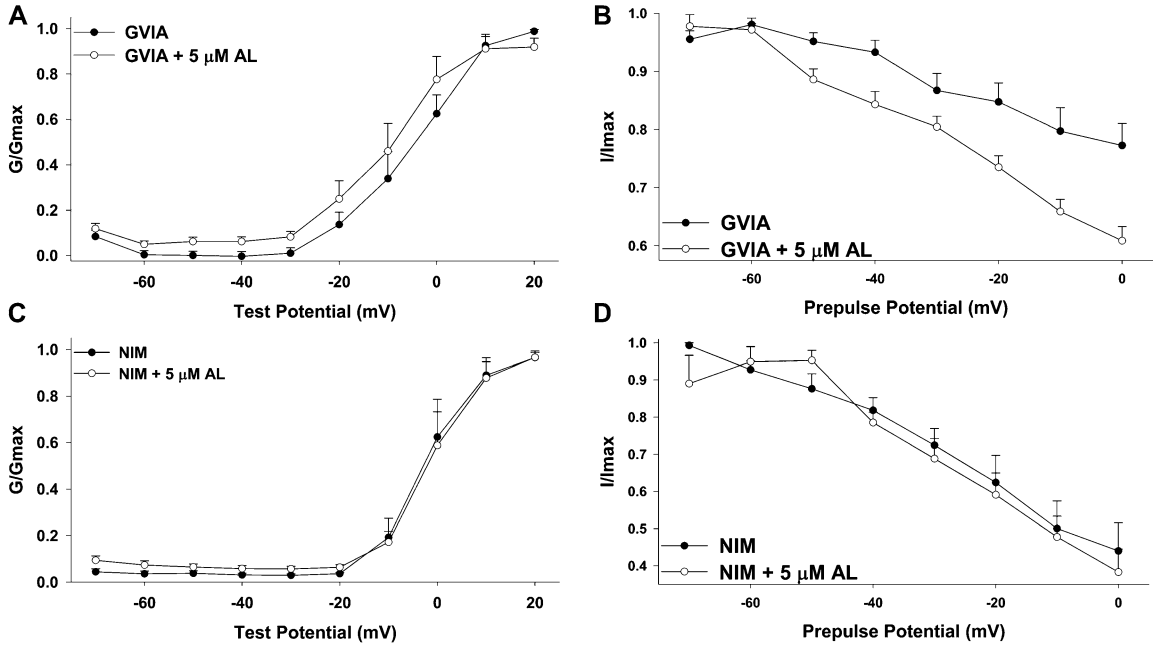

FIG. 6. Allethrin shifts the activation and inactivation of GVIA-insensitive current but does not affect activation or inactivation of NIM-insensitive current. Activation curves (A and C) were generated by normalizing the conductance observed at test pulses from −70 to 20 mV to the maximum conductance. For inactivation curves (B and D) cells were subjected to a 200-ms prepulse of potentials ranging from −70 to 0 mV before testing VGCC current response at 0 mV. Inactivation data were normalized to the maximum current. A clear shift in activation and inactivation is present in GVIA-treated cells exposed to AL (also see Tables 1 and 2). These shifts are likely mediated by L-type VGCCs, as they are absent when cells are treated with the L-type inhibitor, NIM.

current magnitude and slowed its decay but had no effect on peak current of either TTX-sensitive or TTX-insensitive VGSCs (Ginsburg and Narahashi, 1999). In contrast, we observed a pronounced effect of AL on peak Ca^{2+} current, even in the presence of TTX (Fig. 1). Furthermore, this effect was abolished by addition of 100μM Cd^{2+} to the extracellular solution (Fig. 1), confirming that this current is mediated by VGCCs.

Our work contrasts with a previous report showing that AL inhibits recombinant VGCCs in HEK293 cells (Hildebrand *et al*., 2004). Hildebrand *et al.* observed that AL inhibited L-, P/Q-, and T-type VGCCs with EC_{50} values ranging from 6.7 to 7.0μM. Although our concentration, 5μM AL, was slightly below these EC_{50} values, we did not observe evidence of composite VGCC inhibition at 20μM AL (Fig. 1). If anything, there may be a concentration-dependent increase by AL. Interestingly, our results show a similar shift in the inactivation potentials for L-type current during AL exposure (Fig. 6), but Hildebrand *et al.* (2004) did not report a shift in the V_{50} of activation.

One explanation for the differences between our findings and those of Hildebrand *et al.* (2004) is that the subunit composition of the recombinant VGCCs used in their study and the native VGCCs in our study may be different. Hildebrand *et al.* (2004) used a combination of rat α_{1A}(P/Q), α_{1C}(L). or α_{1G}(T) combined with the β_{1b} and $\alpha_2\delta$ subunits. Although the α-subunit composition would remain the same, PC12 cells may express different β subunits in native VGCCs. PC12 cells express β_1, β_2, and β_3 messenger RNA, and different β subunits were shown to associate in the native N-type channel (Liu *et al*., 1996). Additionally, the β subunit can undergo extensive posttranslational modification, resulting in numerous splice variants (Takahashi *et al*., 2003). The β subunit in VGCCs has direct effects on VGCC inactivation, with VGCCs containing the β_{2a} subunit exhibiting slower inactivation than those containing the β_{1b} or β_3 subunit (Olcese *et al*., 1994; Stea *et al*., 1994; Takahashi *et al*., 2003). Furthermore, the identity of the β subunit can shift the I-V curves of VGCC currents, with P/Q-type VGCCs containing β_4 exhibiting peak current at more hyperpolarized potentials than β_{1b}, β_{2a}, or β_3, (Stea *et al*., 1994). Interestingly, the effects of pyrethroids on VGSCs can be modulated by the identity of the VGSC β subunit (Meacham *et al*., 2008), so it is feasible that VGCC effects may also be modulated by subunit composition. This not only highlights the possibility that recombinant cell systems may miss neurotoxic effects because of VGCC subunit heterogeneity, but it also suggests that AL can differentially affect specific VGCCs based on their β-subunit composition.

Another potential explanation for differences between the findings of the current study and the findings of previous studies is that VGCC sensitivity to pyrethroids may be modulated by the phosphorylation state of the channel. A recent study observed that DM, a type II pyrethroid, differentially modulated recombinant N-type VGCCs based on

channel phosphorylation status at the T422 residue (Clark and Symington, 2008). Phosphorylation at this residue under normal conditions results in heightened channel activity and is mediated by protein kinase C (Zamponi *et al*., 1997). Clark and Symington (2008) observed that exposure of N-type VGCCs with a mutation at T422 that mimics phosphorylation resulted in channel activation, whereas wild-type channels are inhibited by DM. Although currently no studies have examined the effect of type I pyrethroids on this mutant channel, this study raises the interesting possibility that pyrethroids exhibit phosphorylation-specific sensitivity.

All the work in this study was performed at room temperature, roughly 25°C. It is well established that the effects of AL on VGSCs show a negative temperature-dependence, contributing to the safe use of pyrethroids around mammals (Ginsburg and Narahashi, 1999; Wang *et al*., 1972). Thus, it is possible that some of the effects we have observed may be lessened at mammalian physiological temperatures. However, not all the effects of AL on VGSCs in rat DRG neurons exhibited a strict dependence on temperature (Ginsburg and Narahashi, 1999). Thus, not all the effects of AL may be temperature-dependent in mammalian neurons.

Our data strongly indicate that AL differentially modulates VGCC subtypes. The work of Meyer and Shafer (2006) indicated that the type I pyrethroid permethrin may act on synaptic VGCCs to increase action potential–independent mEPSCs (Meyer and Shafer, 2006). However, the effect of permethrin on mEPSCs persisted in the presence of ω-conotoxin MVIIC, an antagonist of N- and P/Q-type VGCCs, suggesting that either permethrin was acting on a different VGCC subtype (Meyer and Shafer, 2006) or acting beyond Ca^{2+} entry. The main types of VGCCs found at presynaptic terminals are N-, P/Q-, and R-type (Reid *et al*., 2003). Thus, permethrin might be more effective against R-type VGCCs than other synaptically expressed VGCCs, or there might be a different complement of β subunits. The data presented here indicate that a non-N-type VGCC subtype is strongly stimulated by AL exposure, increasing peak, end, and tail current magnitudes (Fig. 5). Blocking L-type VGCCs with NIM revealed that AL interaction with L-type VGCCs is responsible for the shift in end and peak I-V curves as well as a shift in voltage-dependent inactivation and activation (Figs. 5 and 6), but the identity of the subtypes that are stimulated by AL is not clear. PC12 cells are not known to exhibit high levels of R-type VGCCs (Liu *et al*., 1996), and our analysis of composite VGCC currents indicates that R-type current, if present, at best accounts for less than 20% of total VGCC currents. Thus, in our cells, AL is likely most effective against L-type VGCCs. Further pharmacological studies will indicate whether this is the case.

Pyrethroids are one of the most extensively used classes of pesticides worldwide (Zaim and Jambulingam, 2010) and are used both indoors and outdoors. Increased use of pyrethroids as a result of reduced use of chlorinated pesticides has resulted in increased human exposure (Power and Sudakin, 2007). As a result of widespread applications, pyrethroid metabolites have been found in all populations, including children and pregnant women (Naeher *et al*., 2010; Ostrea *et al*., 2009; Riederer *et al*., 2009). Although the long-term consequences of pyrethroid exposure are not well understood, several studies have described developmental neurotoxic effects in rats during chronic exposure paradigms (Shafer *et al*., 2005b). Pyrethroids are readily metabolized in mammals, but even transient developmental exposure to AL can cause lasting neurobehavioral deficits in mice and alter neurotransmitter receptor levels (Ahlbom *et al*., 1994; Eriksson and Talts, 2000; Shafer *et al*., 2005b). The underlying mechanisms for the developmental effects of AL exposure remain unknown. Our studies suggest that AL differentially modulates VGCC subtypes, which may interfere with normal neuronal development. These findings strongly recommend further characterization of the effect of AL on VGCC function to determine the potential for risks associated with ubiquitous pyrethroid exposure.

FUNDING

National Institutes of Health (R01ES03299).

ACKNOWLEDGMENTS

We thank Ms Sara Fox and Dr Ravindra Hajela of the Department of Pharmacology and Toxicology at Michigan State University (MSU) for assistance with PC12 cell cultures. We also thank Dr Timothy J. Shafer of the U.S. Environmental Protection Agency, Research Triangle Park, NC, for helpful advice regarding the work and Dr M. L. Contreras, formerly of Michigan State University, for the gift of PC12 cells and mouse 7s NGF.

REFERENCES

Ahlbom, J., Fredriksson, A., and Eriksson, P. (1994). Neonatal exposure to a type-I pyrethroid (bioallethrin) induces dose-response changes in brain muscarinic receptors and behavior in neonatal and adult mice. *Brain Res.* **645,** 318–324.

Catterall, W. A., Cestele, S., Yarov-Yarovoy, V., Yu, F. H., Konoki, K., and Scheuer, T. (2007). Voltage-gated ion channels and gating modifier toxins. *Toxicon* **49,** 124–141.

Clark, J. M., and Symington, S. B. (2008). Neurotoxic implications of the agonistic action of CS-syndrome pyrethroids on the N-type $Ca_v2.2$ calcium channel. *Pest Manag. Sci.* **64,** 628–638.

del Toro, R., Levitsky, K. L., Lopez-Barneo, J., and Chiara, M. D. (2003). Induction of T-type calcium channel gene expression by chronic hypoxia. *J. Biol. Chem.* **278,** 22316–22324.

Department of Health and Human Services. (2009). Fourth national report on human exposure to environmental chemicals. Available at: http://www.cdc.gov/exposurereport/pdf/FourthReport.pdf. Accessed May 20, 2010.

Eriksson, P., and Talts, U. (2000). Neonatal exposure to neurotoxic pesticides increases adult susceptibility: A review of current findings. *Neurotoxicology* **21,** 37–47.

Garber, S. S., Hoshi, T., and Aldrich, R. W. (1989). Regulation of ionic currents in pheochromocytoma cells by nerve growth-factor and dexamethasone. *J. Neurosci.* **9,** 3976–3987.

Ginsburg, K., and Narahashi, T. (1999). Time course and temperature dependence of allethrin modulation of sodium channels in rat dorsal root ganglion cells. *Brain Res.* **847,** 38–49.

Hildebrand, M. E., McRory, J. E., Snutch, T. P., and Stea, A. (2004). Mammalian voltage-gated calcium channels are potently blocked by the pyrethroid insecticide allethrin. *J. Pharmacol. Exp. Ther.* **308,** 805–813.

Liu, H., Felix, R., Gurnett, C. A., De Waard, M., Witcher, D. R., and Campbell, K. P. (1996). Expression and subunit interaction of voltage-dependent Ca^{2+} channels in PC12 cells. *J. Neurosci.* **16,** 7557–7565.

Meacham, C. A., Brodfuehrer, P. D., Watkins, J. A., and Shafer, T. J. (2008). Developmentally-regulated sodium channel subunits are differentially sensitive to α-cyano containing pyrethroids. *Toxicol. Appl. Pharmacol.* **231,** 273–281.

Meyer, D. A., and Shafer, T. J. (2006). Permethrin, but not deltamethrin, increases spontaneous glutamate release from hippocampal neurons in culture. *Neurotoxicology* **27,** 594–603.

Naeher, L. P., Tulve, N. S., Egeghy, P. P., Barre, D. B., Adetona, O., Fortmann, R. C., Needham, L. L., Bozeman, E., Hilliard, A., and Sheldon, L. S. (2010). Organophosphorus and pyrethroid insecticide urinary metabolite concentrations in young children living in a southeastern United States city. *Sci. Total Environ.* **408,** 1145–1153.

Narahashi, T. (1986). Toxins that modulate the sodium-channel gating mechanism. *Ann. N.Y. Acad. Sci.* **479,** 133–151.

Olcese, R., Qin, N., Schneider, T., Neely, A., Wei, X. Y., Stefani, E., and Birnbaumer, L. (1994).The amino-terminus of a calcium channel β subunit sets rates of channel inactivation independently of the subunits effect on activation. *Neuron* **13,** 1433–1438.

Ostrea, E. M., Jr, Bielawski, D. M., Posecion, M. C., Jr, Corrion, M., Villanueva-Uy, E., Bernardo, R. C., Jin, Y., Janisse, J. J., and Ager, J. W. (2009). Combined analysis of prenatal (maternal hair and blood) and neonatal (infant hair, cord blood and meconium) matrices to detect fetal exposure to environmental pesticides. *Environ. Res.* **109,** 116–122.

Power, L. E., and Sudakin, D. L. (2007). Pyrethrin and pyrethroid exposures in the United States: A longitudinal analysis of incidents reported to poison centers. *J. Med. Toxicol.* **3,** 94–99.

Ray, D. E., and Fry, J. R. (2006). A reassessment of the neurotoxicity of pyrethroid insecticides. *Pharmacol. Ther.* **111,** 174–193.

Reid, C. A., Bekkers, J. M., and Clernents, J. D. (2003). Presynaptic Ca^{2+} channels: A functional patchwork. *Trends Neurosci.* **26,** 683–687.

Riederer, A., Smith, K., Barr, D., Hayden, S., Hunter, R., and Ryan, P. (2009). Current and historically used pesticides in residential soil from 11 homes in Atlanta, Georgia, USA. *Arch. Environ. Contam. Toxicol.* **58,** 908–917.

Shafer, T. J. (1998). Effects of Cd^{2+}, Pb^{2+} and CH_3Hg^+ on high voltage-activated calcium currents in pheochromocytoma (PC12) cells: Potency, reversibility, interactions with extracellular Ca^{2+} and mechanisms of block. *Toxicol. Lett.* **99,** 207–221.

Shafer, T. J., and Atchison, W. D. (1991). Transmitter, ion channel and receptor properties of pheochromocytoma (PC12) cells - A model for neurotoxicological studies. *Neurotoxicology* **12,** 473–492.

Shafer, T. J., Bushnell, P. J., Benignus, V. A., and Woodward, J. J. (2005a). Perturbation of voltage-sensitive Ca^{2+} channel function by volatile organic solvents. *J. Pharmacol. Exp. Ther.* **315,** 1109–1118.

Shafer, T. J., and Meyer, D. A. (2004). Effects of pyrethroids on voltage-sensitive calcium channels: A critical evaluation of strengths, weaknesses, data needs, and relationship to assessment of cumulative neurotoxicity. *Toxicol. Appl. Pharmacol.* **196,** 303–318.

Shafer, T. J., Meyer, D. A., and Crofton, K. M. (2005b). Developmental neurotoxicity of pyrethroid insecticides: Critical review and future research needs. *Environ. Health Perspect.* **113,** 123–136.

Stea, A., Tomlinson, W. J., Soong, T. W., Bourinet, E., Dubel, S. J., Vincent, S. R., and Snutch, T. P. (1994). Localization and functional-properties of a rat brain α_{1A} calcium-channel reflect similarities to neuronal Q-type and P-type channels. *Proc. Natl. Acad. Sci. U.S.A.* **91,** 10576–10580.

Symington, S. B., Frisbie, R. K., Kim, H. J., and Clark, J. M. (2007a). Mutation of threonine 422 to glutamic acid mimics the phosphorylation state and alters the action of deltamethrin on $Ca_v2.2$. *Pestic. Biochem. Physiol.* **88,** 312–320.

Symington, S. B., Frisbie, R. K., Lu, K. D., and Clark, J. M. (2007b). Action of cismethrin and deltamethrin on functional attributes of isolated presynaptic nerve terminals from rat brain. *Pestic. Biochem. Physiol.* **87,** 172–181.

Takahashi, S. X., Mittman, S., and Colecraft, H. M. (2003). Distinctive modulatory effects of five human auxiliary β_2 subunit splice variants on L-type calcium channel gating. *Biophys. J.* **84,** 3007–3021.

Tatebayashi, H., and Narahashi, T. (1994). Differential mechanism of action of the pyrethroid tetramethrin on tetrodotoxin-sensitive and tetrodotoxin-resistant sodium-channels. *J. Pharmacol. Exp. Ther.* **270,** 595–603.

Tillar, R., Shafer, T. J., and Woodward, J. J. (2002). Toluene inhibits voltage-sensitive calcium channels expressed in pheochromocytoma cells. *Neurochem. Int.* **41,** 391–397.

U.S. Environmental Protection Agency. (2006a). Permethrin facts (reregistration eligibility decision fact sheet). Available at: http://www.epa.gov/oppsrrd1/REDs/factsheets/permethrin_fs.htm. Accessed May 20, 2010.

U.S. Environmental Protection Agency. (2006b). Reregistration eligibility decision for cypermethrin. Available at: http://www.epa.gov/oppsrrd1/REDs/cypermethrin_red.pdf. Accessed May 20, 2010.

Vais, H., Williamson, M. S., Devonshire, A. L., and Usherwood, P. N. (2001). The molecular interactions of pyrethroid insecticides with insect and mammalian sodium channels. *Pest Manag. Sci.* **57,** 877–888.

Wang, C. M., Narahashi, T., and Scuka, M. (1972). Mechanism of negative temperature coefficient of nerve blocking action of allethrin. *J. Pharmacol. Exp. Ther.* **182,** 442–453.

Zaim, M., and Jambulingam, P. (2010). Global insecticide use for vector-borne disease control. World Health Organization, Geneva, Switzerland. Available at: http://whqlibdoc.who.int/HQ/2007/WHO_CDS_NTD_WHOPES_GCDPP_2007.2_eng.pdf. Accessed May 20, 2010.

Zamponi, G. W., Bourinet, E., Nelson, D., Nargeot, J., and Snutch, T. P. (1997). Crosstalk between G proteins and protein kinase C mediated by the calcium channel α_1 subunit. *Nature* **385,** 442–446.